# Serrate–Notch signaling defines the scope of the initial denticle field by modulating EGFR activation

James W. Walters[a], Claudia Muñoz[b], Annalise B. Paaby[a], Stephen DiNardo[a],*

[a]Department of Cell and Developmental Biology, The University of Pennsylvania Medical Center, 421 Curie Blvd., BRB II/III, Room 1215, Philadelphia, PA 19104-6058, USA
[b]Weill Graduate School of Medical Sciences, New York, NY 10021, USA

## Abstract

The Drosophila embryonic epidermis has been a key model for understanding the establishment of cell type diversity across a cellular field. During segmental patterning, distinct signaling territories are established that employ either the Hedgehog, Spitz, Serrate or Wingless ligands. How these pathways control segmental pattern is not completely clear. One major decision occurs as cells are allocated to differentiate either smooth cuticle or denticle type cuticle. This allocation is based on competition between Wingless signaling and Spitz, which activates the Epidermal Growth Factor Receptor (EGFR). Here we show that a main role for Serrate-Notch signaling is to adjust the Spitz signaling domain. Serrate accomplishes this task by activating Notch in a discrete domain, the main purpose of which is to broaden the spatially regulated expression of Rhomboid. This adjusts the breadth of the source for Spitz, since Rhomboid is necessary for the production of active Spitz. We also show that the Serrate antagonist, *fringe*, must temper Notch activity to insure that the activation of the EGFR is not too robust. Together, Serrate and Fringe modulate Notch activation to generate the proper level of EGFR activation. If Serrate-Notch signaling is absent, the denticle field narrows while the smooth cell field expands, as judged by the expression of the denticle field determinant Ovo/Shaven baby. This establishes one important role for the Serrate signaling territory, which is to define the extent of denticle field specification.
© 2005 Elsevier Inc. All rights reserved.

*Keywords:* Segment pattern; Serrate notch; Fringe; Epidermal growth factor receptor; Ovo

## Introduction

The development of embryos, tissues, and organs requires the specification of proper cell types in their proper positions out of an initially unpatterned field of cells. In principle, this can occur by changing the unpatterned tissue into its final pattern all at once by way of a morphogen gradient. Alternatively, the proper constellation of cell types might arise in steps, as a consequence of successive embellishments to an initially coarse pattern. In practice, a combination of both mechanisms likely plays out in most tissues. The *Drosophila* embryonic epidermis has been a key model for understanding how conserved organizer signals pattern cellular fields and has revealed how a stepwise progression from coarse-grained to refined pattern can take place.

In this system, the organizer is defined by Hedgehog (Hh)- and Wingless (Wg)-expressing cells, which line the anterior and posterior edges of each parasegment, respectively. The parasegment is the developmental unit of the segment, and cells in the parasegment are allocated to form each anatomical segment (Martinez Arias, 1993). An important recent discovery was that the organizing signals, Wg and Hh, do not act directly to control the fine elements of segmental pattern but rather control the establishment of smaller signaling territories (Alexandre et al., 1999; Gritzan et al., 1999; Wiellette and McGinnis, 1999; Hatini and DiNardo, 2001a,b). These territories each guide part of the overall patterning that takes place across the cellular field. For example, one major patterning decision across a parasegment is whether to elaborate smooth cuticle or cuticle decorated with denticles. To accomplish this, two

major signaling territories are established: one guided by Wg itself and one by EGFR activation (O'Keefe et al., 1997; Szüts et al., 1997; Payre et al., 1999). Wg and EGFR activity compete for allocation of smooth or denticle producing fates, respectively. The competition plays out in the spatially regulated expression of the zinc-finger transcription factor encoded by the *ovo/shaven baby* locus (called *ovo*, henceforth). *ovo* is necessary and sufficient to specify denticle fate, and it is induced by EGFR activity and repressed by Wg (Payre et al., 1999). While recent analysis has focused on how the domain of Wg signaling activity is modulated (Dubois et al., 2001), here we investigate controls over the EGFR domain of activity.

While Wg and EGFR signaling zones are crucial for the smooth versus denticle decision, there are actually (at least) four signaling territories established by Wg and Hh for proper patterning. The pattern itself consists of not just smooth versus denticulate cuticle, but there is also an elaborate pattern among cells bearing denticles (see diagram Fig. 1). For instance, of fifteen rows of cells across a parasegment, seven rows will produce denticles, but cells along any single row often have similar characteristics. The first row denticles always point to the anterior, while the next rows, row 2 and row 3, point posteriorly, before row 4 points again anteriorly, etc. While it is not yet clear how this refined pattern is specified, the territorial signals (Fig. 1) must play a key role.

Negative regulation by Hh and Wg defines the anterior and posterior boundaries, respectively, of the *Serrate* (*Ser*)
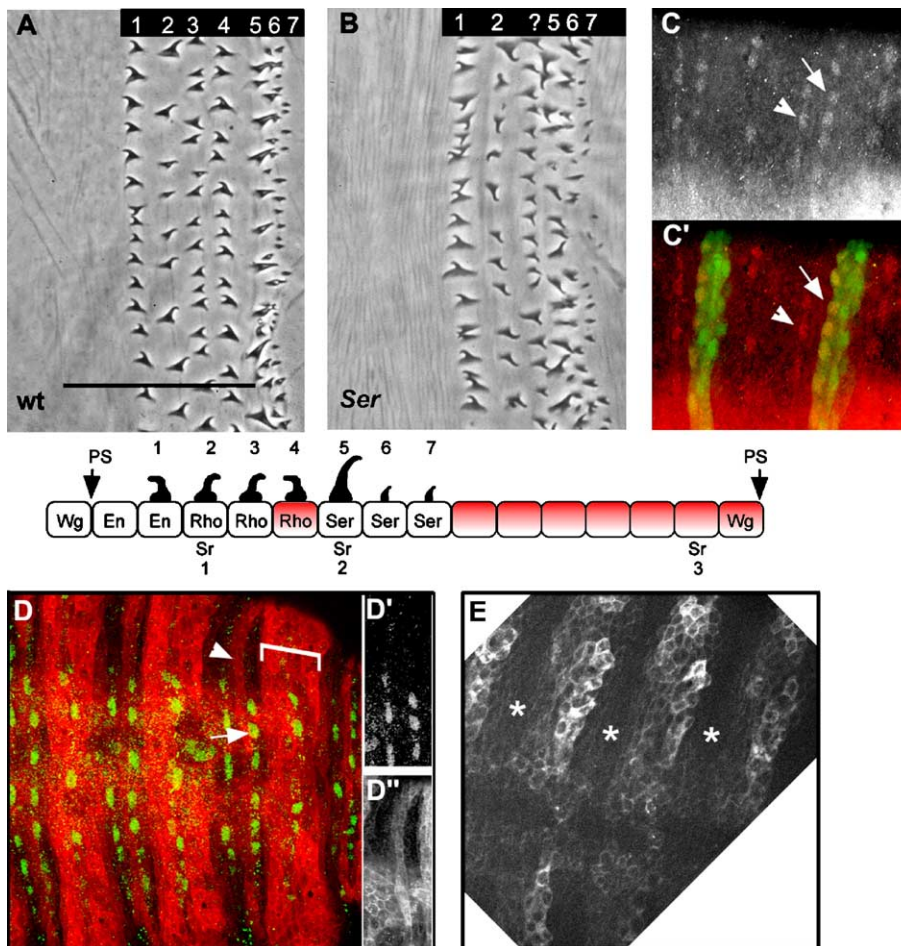


Fig. 1. Notch activity is dependent on Serrate for row type 4 fate. (A) Wild-type cuticle pattern, denticle rows marked 1–7. Rows 1 and 4 point anteriorly; rows 2 and 3 point posteriorly; row 5 denticles are larger and point posteriorly; row 6 and 7 denticles more closely spaced, smaller, and have no obvious orientation. Below this panel is a schematic of the denticle field, with gene expression territories marked (Wg, En/Hh, Rho/sSpi, Ser), as well as the cells expressing the positional marker, Stripe (Sr). PS, parasegment. (B) *Ser^Rx82* mutant shows one row (3 or 4) missing; the row at this position has ambiguous polarity. (C) Anti-Stripe (white); prospective denticle rows 2 and 5 marked with arrow and arrowhead, respectively; see Hatini and DiNardo (2001a,b) for mapping. (C′) Anti-Stripe (red), anti-LacZ (green) double staining of stage 14/15 embryo containing a *Ser–LacZ* reporter transgene; two segments are shown. (D) Notch activation visualized by the mβ-CD2 reporter (red); Stripe (green) is used as a registration marker. mβ-CD2 places the CD2 membrane protein under the control of a suppressor of hairless-dependent promoter, mβ. The single channel insets, panels D′ and D″, focus on one prospective denticle field showing Stripe (D′) or mβ-CD2 (D″). Notch is activated in a broad band (bracket) posterior to prospective denticle field row 5 (arrow, D) and extends past the third row of Stripe-expressing cells. The anterior portion of the broad domain could overlap with a *Ser*-expressing cell. Anterior to prospective denticle field row 5, Notch is also activated in a discrete band of cells (arrowhead and inset D″). (E) Notch activation in a *Ser^Rx82* mutant embryo; single channel of mβ-CD2 shown. Note the absence of the discrete stripe of Notch activity (*). Scale bar is 50 μm in panels A, B, C, and C′; 100 μm in panels D–E.

domain (Alexandre et al., 1999; Gritzan et al., 1999; Wiellette and McGinnis, 1999). Ser is a membrane bound ligand for the Notch receptor, which itself is not spatially regulated but expressed on all cells across the parasegment. At the same time, Hh signaling induces *rhomboid* (*rho*) expression in two cells (Alexandre et al., 1999) posterior to the Engrailed (En) cells (the source of Hh). *rho* expression is the limiting factor in causing EGFR activation, because Rho is responsible for processing the full-length, inactive Spitz (mSpi) into the cleaved, active, and secreted form of the protein, sSpi (Lee et al., 2001; Tsruya et al., 2002). Like Notch, the expression of mSpi and the EGFR are not spatially regulated and are expressed on all cells. Thus, wherever and whenever *rho* is expressed, an EGFR signaling source is established.

The main source for sSpi production is established just posterior to the Hh-expressing domain. While Hh induces *rho* in two rows of cells posterior to the En cells, apparently this is not sufficient for the normal pattern, because an additional line of *rho*-expressing cells is induced just posterior to the Hh-dependent *rho* domain. This third row of *rho* expression abuts the Ser domain and is in fact induced by Ser–Notch signaling (Alexandre et al., 1999; Wiellette and McGinnis, 1999). Thus, two different signaling pathways specify the three rows of *rho*-expressing cells. The reason for this added complexity has been unclear. Additionally, after cell differentiation, *Ser* mutant embryos exhibit one less row of denticles per segment (Wiellette and McGinnis, 1999). The reason for this, too, has been unclear.

Our previous work examining the contribution of EGFR signaling to ventral patterning focused on two negative regulators of its action, *yan* (also called *anterior open*) and *argos* (O'Keefe et al., 1997). While Yan is a transcriptional repressor, the action of which is relieved by EGFR activation through MapKinase phosphorylation (Rebay and Rubin, 1995), Argos sequesters the EGFR ligand sSpi (Klien et al., 2004). These elements of EGFR control act downstream of sSpi production. We reasoned that the complexity of *rho* expression might impart a means of fine-tuning EGFR activity upstream of the production of sSpi ligand.

We thus re-investigated the role of Ser-dependent Notch signaling in epidermal patterning and tested for the involvement of a known negative regulator of this pathway, *fringe* (*fng*). We first mapped receptor activation using Notch reporter constructs, localizing Serrate-dependent Notch activation precisely to the cells that induce the third line of *rho* expression. This nicely confirms previous genetic tests and further argues that this induction is direct. In addition, our analysis of *Ser* and *fng* mutants showed decreased and increased levels of EGFR activation, respectively. Furthermore, *fng* mutants exhibited extra denticles, and this phenotype was suppressed by removing one copy of the EGFR gene. This was consistent with increased the EGFR activation we observed for *fng*

mutants. Since *Ser* mutants showed lowered activation of the EGFR, we directly tested for and observed a more narrow specification of the denticle field, and a concomitant increase in the smooth cell field, explaining the *Ser* mutant phenotype. Our results show why two pathways are utilized for the induction of *rho* expression: apparently the Hh-induced specification of *rho* expression is not sufficient for proper width of the denticle field, and Ser–Notch signaling is thus engaged to effect proper patterning. Finally, we further suggest that Fng temporally modulates Ser–Notch activation to ensure proper patterning.

## Materials and methods

### Fly strains

Presumptive null mutations were used for *Ser* and *fng*: $Ser^{Rx82}$ (FBal0030223) and $Ser^{Rx106}$ (FBal0030221), from Sarah Bray, and $fng^{13}$ (FBal0034611), $fng^{80}$ (FBal0034617), and $fng^{80}$ $Ser^{Rx82}$, from Ken Irvine. P{w+; UAS-Rho C1} (Golembo et al., 1996) was recombined onto the *Ser* mutant chromosomes. Stocks were made *yw* and balanced over TM6 B Tb P{w+; y+} for cuticle analysis or TM3 Sb P{w+; Ubx-LacZ} for gene expression analysis. To reduce the dose of the EGFR in *fng* mutants, we analyzed the progeny of the cross: $EGFR^{top-co}$/CyO P{w+; Act5C-GFP}; $fng^{13}$/MKRS to CyO/Sp; $fng^{80}$/TM3 P{w+; Ubx-LacZ}. GFP+ and GFP− embryos were sorted using a fluorescent stereo microscope separately onto plates, aged and prepared for cuticle analysis. The fraction of embryos that were phenotypically *fng* was tabulated. To test for rescue of row four denticles, progeny of the following cross, raised at either 18 or 29°C, were examined: *yw*; P{w+; UAS-Rho C1} $Ser^{Rx106}$/TM6 B Tb {Pw+; y+} to *yw*; P{w+; Ptc-GAL4}; $Ser^{Rx82}$/TM6 B Tb {Pw+; y+}. P{w+; Ser–LacZ II-9.5} was a gift from Eli Knust (Bachmann and Knust, 1998). P{w+; E(spl)mbeta-CD2} was from Sarah Bray (de Celis et al., 1998). Su(H) binding sites-LacZ were described by Go and Artavanis-Tsakonas (1998).

### Cuticle preparation, immunohistochemistry, and in situ hybridization

Embryos were collected on apple agar plates, aged for the appropriate time, and either processed to visualize cuticle pattern by phase-contrast microscopy (van der Meer, 1977), or fixed and processed for immunofluorescence and/ or in situ hybridization, as described previously (Hatini and DiNardo, 2001a; Hatini et al., 2000). Digoxygenin- or fluorescein-labeled probes for RNA in situ hybridization were made by standard procedures, using a Serrate (Robert Fleming) or Fringe (Ken Irvine) cDNA, in pBS (KS+), or Ovo cDNA LD47350 (from DGC 1.0) in pOT2. The Serrate/fringe double label RNA in situ used digoxygenin- and fluorescein-labeled RNA probes, respectively, and was

visualized by alkaline phosphatase (NBT/BCIP) followed by Fast Red (Vector Labs) histochemistry. The ovo labeling was visualized by Tyramide Signal Amplification (TSA, NEN), using a digoxygenin-labeled Ovo probe, followed by anti-digoxygenin coupled to HRP, and then 15 min tyramide–fluorescein incubation.

The following antibodies (and dilutions) were used: guinea pig anti-Sr (1:500, a gift from T. Volk), rabbit anti-Engrailed (1:100, gift from C. H. Girdham and P. H. O'Farrell), anti-dpERK (1:2000, Sigma cat. #M8159), rabbit anti-betagalactosidase (1:2000, Molecular Probes), and anti-phosphotyrosine (1:500, Upstate Cell Signaling, cat. 06-427). Secondary antibodies, used at 1:400, were conjugated to Alexa™ (Molecular probes) or Cy3 and Cy2 dyes (Jackson Labs), biotin (Vector Labs), or horseradish peroxidase (Roche). RNA in situ/antibody multiple labelings were carried out by developing the hybridization signal first, followed by appropriate antibody incubations.

The dpERK signal in the ventral epidermis is relatively low level and was quite variable under our usual fixation conditions. We found empirically that longer fixation times were essential to obtain a reasonably consistent signal. Embryos to be fixed were aged and pre-processed as usual, and then placed in a 1:1 mixture of heptane and 4% formaldehyde, $1\times$ PBS for 2 h at room temperature. Formaldehyde was diluted from a 16% stock (Electron Microscopy Sciences) that had been aliquoted and stored at $-80°C$, though we did not test whether this was necessary. Subsequent de-vitellination and processing were as usual.

## Quantification of signal intensities

For all expression intensity comparisons, the embryos are collected, fixed, and stained in the same tube (they are genotype-marked siblings from the same cross). For signal intensities, standardized stacks confocal $Z$ series were obtained using Zeiss LSM510 software under conditions where the full dynamic range of the detector is utilized. A fixed number of optical sections in the $Z$ plane was used for all samples to ensure that the same amount of tissue depth was measured. Images were gathered using one setting for gain and offset for all measurements. The appropriate sections, which spanned the relevant height of the epidermis, were merged, and the raw channel data were imported into IP Lab for quantification. Areas of interest were selected as indicated in the figures and mean intensities for dpERK or mβ-CD2 signals quantified. For dpERK, the areas of interest were chosen to be off of the midline and also did not include the most lateral portions of the signal that we judged would not contribute to the prospective (ventral) denticle field. The mean for the aggregate signal intensities was tallied. For mβ-CD2, the areas of interest were the narrow band and roughly the first three rows of the broad band.

## Justification for methodology of counting cell types

In order to count cells and their types, we used anti-phosphotyrosine to label cell contours as well as the actin-based protrusions that become denticles. Using such stains, it is unambiguous which cells make up the denticle field (Martinez Arias, 1993; J.P.W. and S.D. unpublished results). The supplemental figure shows both *Ser* mutant embryos as well as their heterozygous sib controls (*Ser*/TM3, P{w+; Ubx-LacZ}). Images were captured essentially as described above. A line was drawn parallel to the midline and crossing the rows of cells in the segment (Supplemental Fig. 1B′). Cells that intersected each line were tallied as denticle or smooth, and such measurements were repeated at up to eight different positions per segment (Supplemental Fig. 1B′, where five such lines are indicated). This process was repeated for three abdominal segments (A4–7) and on several sibling embryos for each genotype, either wild-type heterozygotes (*Ser*/TM3, {Pw+; Ubx-LacZ}) or mutants (*Ser*/*Ser*). The data were reported as the average cell number per segment, per denticle field, or per smooth field. Significance was judged by a Students' $t$ test. To quantify the breadth of the *ovo* expression domain, embryos were also labeled for Ovo RNA and En protein. The *ovo*-expressing cell rows were tallied as above.

## Results

### Serrate is necessary for Notch activation in prospective denticle row four

Removal of *Ser* causes a loss of one row of denticles (cf. Figs. 1A and B; Wiellette and McGinnis, 1999). While denticle rows at the anterior and posterior portions of the denticle field appear normal (rows 1, 2 and 5, 6; cf. Figs. 1A and B), only one row of denticles is elaborated from the region normally comprising denticle rows 3 and 4. Additionally, denticles in this row exhibit defects in shaping, as the hook is now variable. *Ser* is expressed just posterior to the affected region, as visualized by immunostaining embryos containing a *Ser–LacZ* transgene, and using the expression of Stripe protein as a positional marker (Figs. 1C and red in C′). Stripe expression marks prospective denticle row 2 (arrowhead) and 5 (arrow), as well as a third row of cells in the region of the smooth cuticle (Hatini and DiNardo, 2001a,b). Cells making up the anterior border of *Ser* expression will generate denticle row 5 (Fig. 1D, arrow) (Alexandre et al., 1999). Thus, *Ser* is expressed posteriorly adjacent to the rows affected by *Ser* mutants.

The requirement of *Ser* for proper denticle field patterning and the placement of its expression raised a question as to where within the prospective denticle field cells the Notch pathway was activated by Ser. To address this, we used two reporters for Notch activation, mβ-CD2 (de Celis et al., 1998) or Su(H) binding sites-LacZ (Go and

Artavanis-Tsakonas, 1998), to first map where the pathway was activated, and then asked whether the activation was *Ser* dependent. Both Notch reporters showed quite broad domains of activation (Fig. 1D, red; data not shown). In wild-type embryos, high levels of mβ-CD2 expression (Fig. 1D bracket) were observed posterior to prospective denticle row 5 (Fig. 1D, arrow) and thus largely in the area that will differentiate smooth cuticle. This broad domain of Notch activation is largely posterior to the *Ser* expression domain (cf. Figs. 1C, C′, and D). Distinct from this broad domain, there is a discrete band of Notch reporter activity just anterior to prospective denticle row 5 (Figs. 1D, arrowhead, and inset D″). This region is the same as that affected in the *Ser* mutant.

In *Ser* null mutant embryos, this discrete band of Notch activity disappeared (Fig. 1E, asterisk indicates where discrete band should be). These data map a discrete band of *Ser*-dependent Notch activation anterior to the *Ser*-expressing cells. The broad domain of Notch activation was largely unaffected in *Ser* mutants (Fig. 1E), though there may be a slight decrease in the anterior portion of the domain. This broad domain of Notch activation might represent the persistence of earlier Notch activation by Delta during neurogenesis, or alternatively it might represent a late role for Notch pathway activity in the Wg-dependent specification of smooth cuticle (Couso and Martinez-Arias, 1994). We infer from our results that Ser-dependent Notch activation in prospective denticle row 4 is important for proper denticle field patterning. Our positioning of this Ser-dependent Notch activation is consistent with the proposition that Ser is directly responsible for the induction of *rho* expression in these cells (Wiellette and McGinnis, 1999).

*fringe tempers Serrate-mediated Notch signaling in the parasegment*

The glycosyltransferase Fng cell intrinsically modifies the Notch receptor in various tissues (Bruckner et al., 2000; Moloney et al., 2000). As a consequence of this modification, *fng* down-regulates Ser-dependent Notch activation. This suggested to us that *fng* was a candidate for limiting Notch signaling among denticle field cells. *fng* RNA expression is quite dynamic, both temporally and spatially. Temporally, in ventral epidermis, while *Ser* expression emerged during late stage 11 (Figs. 2E and E′, red), *fng* expression did not begin until stage 13 (Figs. 2F and F′, blue); and it persisted through stage 14 while *Ser* expression declined (Figs. 2G and G′). Spatially, *fng* is expressed
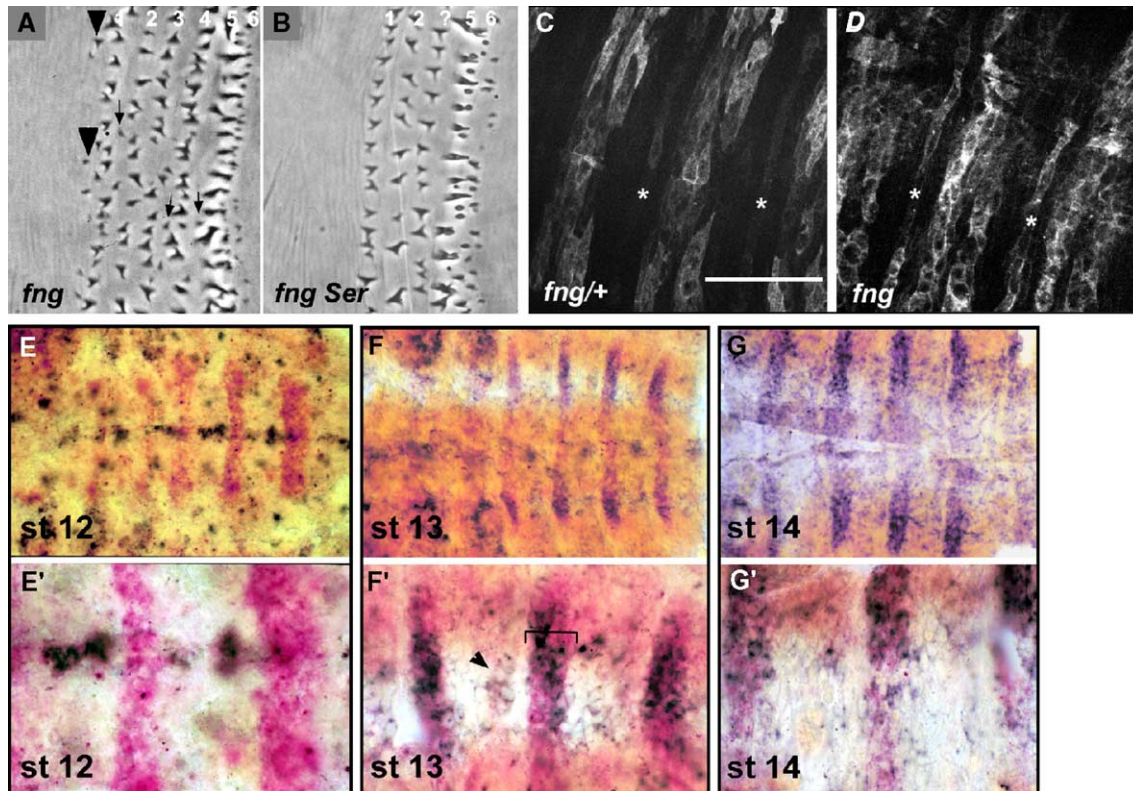


Fig. 2. Fringe regulates Notch signaling in the region signaled by Serrate. (A) *fng^80* mutant shows small extra denticles (arrows) interspersed with the normal pattern of denticles. Additionally extra denticles were seen anterior to row 1 (arrowheads). (B) A *fng^80 Ser^Rx82* double mutant phenocopies *Ser^Rx82* (compare to Fig. 1B). (C) mβ-CD2 Notch reporter activity in heterozygous control sibling embryos, *fng^80*/+. (D) Notch activity is increased in *fng^80* mutant embryos in the Ser-dependent narrow band (compare asterisks, panels C and D). (E–G) *Ser* (red) and *fng* (blue) double RNA in situ at different stages; (E′–G′) magnified views of panels (E–G), respectively. *fng* is expressed in the cells expressing *Ser* (bracket, F′) and in Engrailed cells (arrowhead, F′). Scale bar is 25 μm in panels A and B; 50 μm in panels C, D, E′, F′, and G′; and 150 μm in panels E, F, and G.

largely in *Ser*-expressing cells (bracket, Fig. 2F′, arrow, and data not shown). The striking overlap between *fng* and *Ser* expression suggested that *fng* might modulate Ser–Notch interactions among the denticle field cells sometime after its induction.

Cuticle preparations confirm that *fng* mutants exhibit a denticle phenotype, consistent with a role for modulating Notch activity. In *fng* mutants, small denticles, which lacked orientation, are interspersed with the normally formed denticles of rows 2–4 (Fig. 2A, arrows). This "extra denticle" phenotype appeared opposite to the loss of denticle phenotype seen in *Ser* mutants, and suggested that *fng* was acting through *Ser*.

Given that *fng* is a negative regulator of *Ser* function, we tested whether the extra denticle phenotype of *fng* mutants is due to excess Ser–Notch signaling by removing *Ser* in a *fng* mutant. We found this to be so, as *Ser fng* double mutants showed the same phenotype as the *Ser* single mutants (Fig. 2B). We conclude that *fng* acts to temper *Ser* signaling in the denticle field.

### *fringe is a regulator of Ser-dependent Notch activity*

To test if *fng* could be responsible for down-regulating Notch activity, we quantified Notch activation in *fng* null embryos using the mβ-CD2 Notch reporter (Figs. 2C and C″ and Table 1). For quantification, the mean intensities were tallied for sibling controls and *fng* mutant embryos (for sibling controls we scored the heterozygous siblings, *fng*/+, that are phenotypically wild type, see Materials and methods), by scoring either the discrete Notch reporter stripe, including two cells posterior to it or, separately, the first three rows for the broad band. For both regions, we found that Notch activity is increased (see Table 1). While the mean intensity near the discrete stripe in sibling control embryos was $39 \pm 2.0$, this increased in *fng* mutants to $53 \pm 2$ ($P < 4 \times 10^{-10}$). We conclude that *fng* is necessary to restrict Ser-dependent Notch activation in this discrete stripe, which maps within the prospective denticle field. In *fng* mutants, there was a similarly significant increase in

Table 1
Signal intensities of mβ-CD2 reporter

| | Narrow band[a] | Broad band[b] | P value[c] |
|---|---|---|---|
| WT[d] | $38.8 \pm 2.0$[e] | $59.7 \pm 1.7$ | $P < 4 \times 10^{-10}$ ($n = 10$) |
| *fng 80*[f] | $52.8 \pm 2.1$ | $80.0 \pm 2.6$ | $P < 5 \times 10^{-8}$ ($n = 10$) |

Signal intensities of standardized images were measured on regions of interest using IP Lab software.
[a] Notch reporter activity was estimated by taking measurements for the discrete Ser-dependent band and two rows of cells posterior to this.
[b] Notch reporter activity was estimated by measuring the first three rows of the broad band.
[c] P value as measured by Student's *t* test.
[d] WT = mβ-CD2; *fng [80]*/TM3 Sb P{w+; Ubx-LacZ}. Heterozygous embryos that are phenotypically wild type are designated WT.
[e] Represents Standard Error of the Mean.
[f] mβ-CD2; *fng*[80]. *n* is the number of animals counted.

the region encompassing the broad domain of Notch activation (sibling control, $60 \pm 2$; *fng*, $80 \pm 3$; $P < 5 \times 10^{-8}$). This is consistent with the prospect that some of the broad domain of Notch activation is also *Ser* dependent, since in *Ser* mutants we had noted a slight decrease in the anterior portion of this domain by reporter gene expression (Fig. 1E). Nevertheless, while there might be some contribution to broad domain Notch activation by *Ser*, it is the discrete band that is strikingly Ser dependent and located in the region where *Ser* exhibits its phenotype. While some extra denticles observed in *fng* mutants could be explained directly by the increased Notch activation, *fng* mutants also had small, extra denticles a substantial distance away from the Ser source. Some of these appeared anterior to the normal row 1 (Fig 2A, arrowheads). Since Ser is a membrane-tethered ligand this feature was not easily explained by direct effects on Notch activation. Yet, these ectopic denticles also disappeared in *fng Ser* double mutants (Fig. 2B) demonstrating that they were, at least indirectly, a result of Ser–Notch signaling. Taken together, these data suggested that the extra denticles are due to a change in a relay signal that is affected by Notch activation.

### *Decreased EGFR activity rescues the fringe phenotype*

It is known that Ser–Notch signaling controls the expression of the necessary activator for EGF-activation, *rho* (Alexandre et al., 1999; Wiellette and McGinnis, 1999). In *Ser* mutants, *rho* expression is absent from one row of cells, the posterior-most row of the *rho* domain. This presumably leads to lower overall EGF pathway activation, and consequent loss of a denticle row, although a decrease in dpErk signal has not been documented to date (but see below). Additionally, ectopic activation of the EGFR pathway has been shown to lead to extra denticles (O'Keefe et al., 1997; Szüts et al., 1997). Thus, it is reasonable to suppose that the excess Notch signaling in *fng* mutants led to EGFR overactivation.

As a first test of this possibility, we looked for genetic interactions between *fng* and the EGFR. We sought to lower the amount of EGFR signaling in a *fng* mutant background. If the *fng* phenotype was due to excess EGFR signaling, then removing one copy of *EGFR* might limit the over-activation, thus suppressing the *fng* phenotype. To accomplish this, we scored the penetrance of the *fng* cuticle phenotype among siblings with either normal *EGFR* dose or heterozygous for a null mutation in *EGFR*.

Larvae were scored as having a *fng* phenotype if they had extra denticles anterior to row one and/or extra denticles within the denticle field. Larvae that were wild type at the *EGFR* locus exhibited the *fng* phenotype at approximately the expected Mendelian frequency (11 of 53 cuticles scored, or 20%, which was not statistically different from the expected 25%; $P > 0.5$). Larvae with a reduced gene dose of *EGFR* (*EGFR*/+) exhibited a significantly lower penetrance

of the *fng* phenotype (10 of 70 larvae cuticles scored, or 14%; $P < 0.05$). Thus, lowering the dose of the EGFR suppressed the *fng* mutant phenotype, providing evidence that increased EGFR activation, could account for the extra denticle phenotype of *fng* mutants.

### Loss of fringe corresponds to increased EGFR signaling

The genetic interaction between *fng* and *EGFR* suggested that *fng* mutants have excess EGFR activation, which should lead to excess activation of its downstream components. This was indeed the case. Stage 13 control and sibling *fng* mutant embryos were labeled for activated MapKinase, its di-phosphorylated form, dpERK (Figs. 3C and D, green). *fng* homozygous mutants were identified by loss of the LacZ staining contributed by a *fng+* balancer chromosome (red). In control embryos, we consistently observed two peaks of dpERK accumulation, with variable spreading away from these peaks (Fig. 3C). The first peak overlaps the
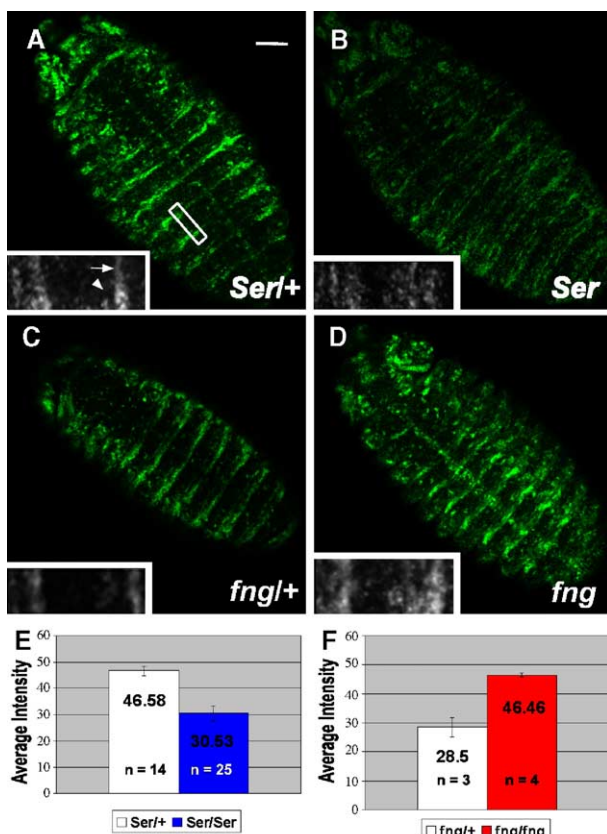


Fig. 3. Loss of Notch pathway components affects EGFR signaling. Ventral view, representative stage 13 embryos with anti-dpERK antibody; insets are magnified views of a two segment region similar to that boxed in panel A. (A) *Ser^Rx106*/+ (TM3 P{w+; Ubx-LacZ}), there are two peaks of dpERK activity per segment (inset arrowhead and arrow). (B) *Ser^Rx106* mutant. (C) *fng^13*/+ (TM3 P{w+; Ubx-LacZ}). (D) *fng^80* mutant. (E and F) Average intensity of dpERK signal in sibling controls (white bars) and *Ser^Rx106* (blue bar) or *fng^80* (red bar) embryos, respectively. Scale bar is 50 μm in panels A–D.

posterior-most En cells, while the second peak was located posterior to the En cells, within the *rho* expression domain (O'Keefe et al., 1997) (and data not shown). Since genetic data suggest that EGFR signaling is necessary for denticle formation across all denticle field cells (O'Keefe et al., 1997; Szüts et al., 1997; Urban et al., 2001), we presume that, as in other tissues, accumulation of dpERK is not sensitive enough to visualize all cells in which the EGFR is activated. Perhaps the variable spreading of signal that we observed represents the lower level of EGFR activation away from these peaks.

To our eye, embryos lacking *fng* showed increased dpERK accumulation in the prospective denticle field. A representative example of wild type (Fig. 3C) shows the lower peak intensity of dpErk stain (green; white in inset) compared to a *fng* mutant sibling (Fig. 3D). Because we find slight variation in dpErk staining intensity in wild-type embryos, especially between stripes, we quantified the dpErk activation across hemisegments in denticle field cells to provide a fair comparison between *fng* mutants (32 hemisegments) and their wild-type siblings (24 hemisegments) (Figs. 3E and F; see Materials and methods). Confocal images were carefully gathered using one setting for gain and offset for all measurements. Additionally, a fixed number of optical sections in the Z plane were used for all samples to ensure that the same amount of tissue depth was measured. The mean intensities for wild-type and mutant embryos were tallied. The mean intensity in dpErk signal in *fng* was greater than that in wild type (*fng*: $47 \pm 1$, $n = 3$, vs. sibling controls: $29 \pm 3$, $n = 4$; $P$ value of $6 \times 10^{-3}$, Students $t$ test). The increase in EGFR pathway activation supports our genetic interaction data. We conclude that *fng*, through its modulation of Notch activity, acts to keep EGFR activity in check across the denticle field.

### Loss of Serrate corresponds to decreased EGFR signaling

Knowing that *rho* expression is reduced in *Ser* mutants we expected that *Ser* embryos should show decreased EGFR signaling. We repeated the assay for EGFR activation in stage 13 *Ser* mutant embryos and observed a decrease in aggregate signal intensity as compared to wild type (Figs. 3A and B green; white in inset). The mean intensity for wild type was significantly higher than that for *Ser* (sibling controls: $47 \pm 2$, $n = 14$, vs. *Ser^Rx82*: $31 \pm 3$, $n = 25$; $P < 1 \times 10^{-10}$, Students $t$ test). Representative examples are shown in Figs. 3A and B. While the width of dpERK activity proved difficult to map at these early stages, we found that the highest peaks of sibling control dpERK activity were reduced in *Ser* mutants. Since the difference in peak intensities were drastically different than sibling controls (Fig. 3E), it is reasonable to suppose that the contours of any signaling downstream of EGFR activation also changed. We conclude that *Ser* is necessary to induce proper EGFR activation in the region affected by the *Ser* phenotype; this

effect is likely through Ser-dependent Notch regulation of *rho* expression.

## *Serrate–Notch signaling does not establish a developmental boundary within the denticle field*

Previous work raised the possibility that Ser–Notch signaling played a different role in denticle patterning. It was noted that the *rho/Ser* gene expression boundary correlated with a flip in denticle polarity (Alexandre et al., 1999). While the denticle tips of row 4 cells hook to the anterior, those of row 5 cells hook posteriorly. This correlation suggested that a developmental boundary, defined by the *rho/Ser* expression interface, might be essential for proper polarity of denticles elaborated on each side of that boundary. Furthermore, it suggested that Ser–Notch activation might be crucial for the establishment of this boundary, and thus for proper denticle polarity. Consistent with this idea, an ambiguous polarity is seen in one row of the *Ser* mutant's denticles (Wiellette and McGinnis, 1999). Since Ser–Notch signaling is clearly important for proper width of the *rho* expression domain, we sought to distinguish whether Ser–Notch signaling was essential for this developmental boundary, and thus denticle polarity, or simply for generating sufficient *rho* expression.

To make this distinction, we re-supplied high level *rho* expression in *Ser* mutant embryos. While we cannot restore *rho* expression selectively in the Ser-dependent portion of its domain, we can utilize a *patched*-Gal4 driver, which expresses at high levels in the first *rho* cell (denticle row 2), gradually decreasing in expression posteriorly from this point, thus covering the full prospective *rho* domain (and beyond). *Ser* null animals that carried a UAS-rho construct under the control of a *patched*-Gal4 driver often exhibited a normally shaped denticle in row 4 (Fig. 4B, and inset). While relatively low level *rho* expression, generated by

raising embryos at 18 or 22°C, rarely restored proper denticle row 4 polarity, restoring higher level *rho* expression, obtained by raising embryos at 29°C, did restore polarity. The expression of *rho* by *patched*-Gal4 led to the expected increase in EGFR activation (as observed by anti-dp-ERK; Fig. 5A), and also an expansion of type 5 denticles posterior to the normal denticle field (Fig. 4B). Thus, Ser–Notch signaling is not obligatory to the establishment or maintenance of a developmental boundary within the denticle field. The main role for Ser–Notch signaling might simply be to allow for *rho* to be expressed to a sufficient degree (see Discussion).

## *Serrate–Notch signaling sets the anterior-posterior extent of the denticle field*

If Ser–Notch signaling does not have a role for this developmental boundary, what is its role? Having documented that Ser-dependent Notch activation affects the levels of EGFR activation in the denticle field (Fig. 3B), we now revisit the question of how the loss of one denticle cell row might arise in *Ser* mutants. In principle, this could be due to proper specification of denticle field size, and then loss of a row due to cell death. Wiellette and McGinnis (1999) had ruled this out, and we also found no evidence for the activation of caspases within denticle field cells (data not shown). Their previous work had considered and dismissed the possibility that a defect in cell proliferation might account for the loss of a denticle row (Wiellette and McGinnis, 1999). We confirmed this by directly counting cells across the parasegment in both wild-type and *Ser* mutant late stage embryos (Figs. 5A–B; Supplementary Fig. 1).

The cells of the ventral epidermis are hexagonally packed, and such overlap at cell edges can confound attempts to estimate the number of rows across a parasegment. To overcome this, we captured images from the
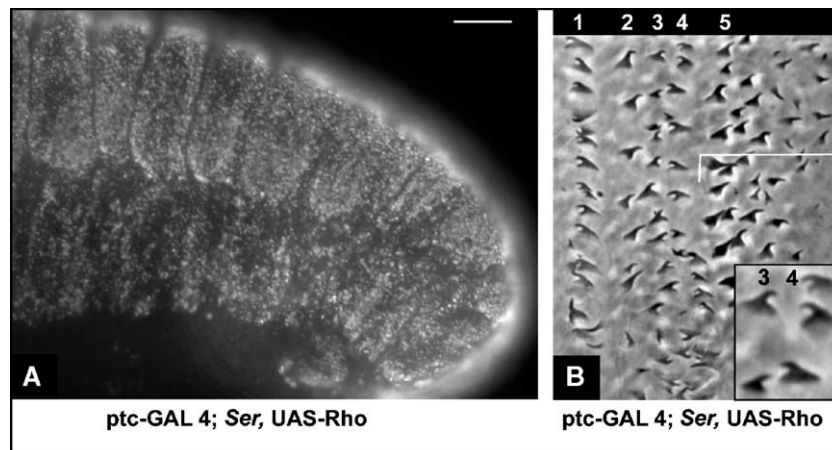


Fig. 4. Re-supplying Rhomboid expression in Serrate mutants restores type 4 denticles. (A) Ptc-GAL4; UAS-rho *Ser*[Rx106]/*Ser*[Rx82] stage 13 embryo labeled with anti-dpERK, lateral view. Expanded activation of EGFR pathway is observed. (B) Restoration of type 4 denticles in ptc-GAL4 driving UAS-rho in a *Ser* background at 29°C. Inset shows magnified types 3 and 4 denticles. Bracket marks posterior expansion of type five denticles. Scale bar is 50 μm in panel A; 5 μm in panel B.
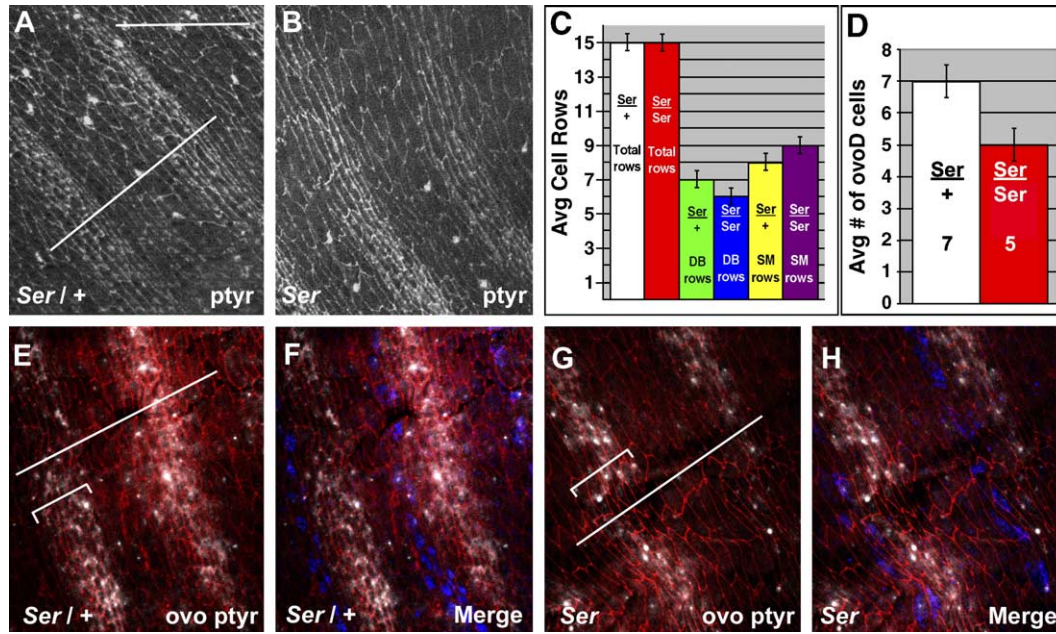
Fig. 5. The denticle field determinant ovo is expressed in fewer cell rows in Serrate mutants. (A and B) Cell counts of stage 14 embryos labeled with anti-phosphotyrosine (white). (A) Representative $Ser^{Rx106}$/+ (TM3 Sb P{w+; Ubx-LacZ}) embryo. An anterior–posterior line was drawn parallel to the midline (see Materials and methods for details), and cells that intersected this line were counted. This was repeated at four positions per hemisegment; one representative line (white) is shown as an example. See Supplementary Fig. 1 for a detailed description of counting. (B) Representative $Ser^{Rx106}$ mutant embryo. (C) Graph of cell counts in sibling controls (white, green, yellow) and Ser mutants (red, blue, purple). "DB", denticle belt; SM, smooth cell types. (D) Graph of Ovo-expressing cell rows in sibling controls (white) and Ser mutants (red). (E–H) In situ of ovo expression (white), together with anti-phosphotyrosine (red) for cell outlines, and the positional marker anti-Engrailed (blue). (E–F) Representative control sibling embryo $Ser^{Rx106}$/+. (E) ovo expression and antiphosphotyrosine. Bracket defines Ovo domain; white line marks midline. (F) Merge of ovo expression, anti-En, and anti-phosphotyrosine. (G–H) Representative $Ser^{Rx106}$ mutant. (G) ovo expression (white) and anti-phosphotyrosine. Bracket defines Ovo domain; white line marks midline. (F) Merge of ovo expression, anti-En, and antiphosphotyrosine. Scale bar is 50 μm in panels A, B, E, and F; 40 μm in G and H.

relevant stage, and drew a line from one parasegment to the next, parallel to the ventral midline (Fig. 5A; Supplementary Fig. 1). We then counted the number of cells that intersected the line across one parasegment and repeated this measurement at three other ventral positions within each hemisegment. Figs. 5A, E, and G and Supplemental Fig. 1, panels B′ and D′, are marked with such a line to help the reader see how we count. The nature of the cell packing means that, for any given line, there might be slightly more or slightly fewer cells crossed, but averaged over a number of such lines per hemisegment we can derive a very good estimate for cell number across the segment. Note that the measurements were carried out on several segments (abdominal segments 4–7) and in several different embryos to arrive at statistical significance. Since the process was carried out identically for the sibling Ser embryos our comparison should reveal any relative change in sibling controls versus Ser. In these cells counts, we were able to tally separately smooth versus denticle field cells, because these cell types are distinguishable at stage 14 (Fig. 5A; Supplementary Fig. 1). First, they exhibit distinct apical contours, with smooth cells being hexagonally shaped and denticle cells being more recti-linear, with narrow antero-posterior extents and elongate dorso-ventral edges (Martinez Arias, 1993). Second, pro-spective denticle cells display actin-based protrusions, which become indelibly marked as denticles after cuticle

deposition. Ser mutants were identified by lack of a marked balancer (TM3 Ubx-Lac Z). There were on average fifteen total cells across each parasegment (Fig. 5C, white vs. red) for both wild-type ($n = 7$ animals) and Ser mutant embryos ($n = 6$ animals), suggesting, again, that there was no proliferation defect nor any increased apoptosis in Ser mutants. In contrast to the equal total cell count, there was, on average, one less row of denticle field cells in Ser mutants ($6 \pm 0.5$, compared to $7 \pm 0.5$ for sibling controls; Fig. 5C, blue vs. green). Finally, one additional smooth cell row is present in Ser mutants at the expense of one denticle-producing row ($9 \pm 0.5$ compared to $8 \pm 0.5$ for sibling controls; Fig. 5C, purple vs. yellow). This analysis was conducted at stage 14 after allocation of the cells in the denticle field was complete. These results suggested that the initial allocation of cells to the denticle field might have been altered in Ser mutants.

To test this directly, we examined the expression of the earliest marker for the denticle field, ovo, a gene that is necessary and sufficient for denticle formation. ovo is expressed at stage 13 and was visualized by fluorescence RNA in situ hybridization (white), while cell counting was facilitated by using an antibody to phosphotyrosine to reveal cell outlines (red), and Engrailed (blue), which was used as a marker for position across the parasegment (Figs. 5F and H). Cell counts were conducted as outlined above. We

observed a decrease in the mean cell number of *ovo*-expressing cells per segment in *Ser* mutants (5 ± 0.5, n = 7 animals) compared to control siblings (7 ± 0.5, n = 11 animals; $P < 8.9 \times 10^{-6}$). We conclude that Ser–Notch signaling sets the width of the EGFR activation domain (by its regulation of *rho* expression), and the EGFR activation domain consequently sets the width of the *ovo* expression domain. Without *Ser* function, roughly one less denticle row is specified.

## Discussion

In patterning the ventral epidermis, four signaling pathways are involved, each activated by signals emitted from defined territories (O'Keefe et al., 1997; Szüts et al., 1997; Alexandre et al., 1999; Gritzan et al., 1999; Wiellette and McGinnis, 1999; Hatini and DiNardo, 2001a,b). Here we resolve why the Notch pathway, activated by Ser, is utilized, demonstrating that it is necessary to specify the correct number of denticle field rows. Notch signaling accomplishes this task indirectly, by modulating the extent of EGFR activation across the parasegment. This is realized by the induction of an extra stripe of *rho*-expressing cells. This additional line of *rho* is necessary for high enough levels of EGFR activation to appropriately widen the zone of expression of the denticle field determinant *ovo*.

The expression of *ovo* occurs as a consequence of competition between Wg and EGFR pathway activation (Payre et al., 1999). Our data show that the system must also be balanced to assure a proper outcome of the Wg/EGFR competition. In this regard, two separate pathways, Hh and Notch, are used to induce *rho* expression (Alexandre et al., 1999; Wiellette and McGinnis, 1999). These signaling pathways are not redundant with each other in this role but rather assure that *rho* comes to be expressed in three rows of cells—prospective denticle rows two through four.

Hh induces the first two stripes of *rho* expression but does not induce the third (Alexandre et al., 1999). This is curious; since Hh signaling appears to reach that far, as at this position it appears to set the anterior border of *Ser* expression (by repression). An explanation of why Hh is not required for the third stripe of *rho* expression may lay in the fact that *rho* is at its highest level of expression in this row. Since this is furthest from the Hh source, perhaps Hh signaling is not strong enough at this distance to induce *rho* to this high level, and thus Ser-dependent Notch signaling is recruited for this purpose. The outcome of using two pathways to induce *rho* expression is then a wider Rho domain and proper denticle field size.

### Serrate–Notch signaling and specification of field size

The use of Ser, then, is essential to set the proper distance over which the EGFR is activated. Previous work from our

lab demonstrated a similar role for Ser–Notch signaling in setting proper distances—in that instance, it is the distance between muscle attachment cells. The specification of muscle attachment tendon cells, visualized by the expression of Stripe, occurs at defined intervals across each parasegment (Volk, 1999). We showed that Ser-dependent Notch signaling does not determine whether a tendon cell is specified but rather where it is specified. In *Ser* mutants, the proper number of tendon cells appears, but one is specified a single cell row more anteriorly than normal (Hatini and DiNardo, 2001a,b). We draw from these two examples that the main role for Ser–Notch signaling during ventral patterning is to adjust field sizes.

Here, in our analysis of *Ser* mutants, we found that the total number of cells across the parasegment remains the same as in wild type, while there was one fewer row allocated to the denticle field. However, if this is the only effect of losing *Ser*, it is curious that row 3/4 is specifically affected. One inference we draw from this is that whatever mechanisms account for the patterning of row 1, perhaps row 2, and certainly rows 5–7, these mechanisms are unaffected in *Ser* mutants. What is changed is where rows 5–7 are specified, as these more posterior rows must now be specified from more anterior cell rows. Thus, in *Ser* mutants, denticle cell type 5 now differentiates from cell row 4 within the prospective denticle field; similarly, denticle cell type 6 now differentiates from cell row 5. This shift is in concert with the shift in tendon cell specification we reported earlier (Hatini and DiNardo, 2001a,b). What still must be accounted for is why denticle cell type 4 is not specified from cell row 3, but rather is lost. One possibility for the focus of this effect on row 3/4 is that perhaps these two cell rows require the highest level of EGFR activation and thus cannot differentiate properly under the conditions of the lowered level of EGFR activation that we observed in *Ser* mutants. This is supported by the fact that there is proper differentiation of row 3/4 when we re-supplied *rho* to *Ser* mutants. The patterning shift also does not simply predict the assignment of ambiguous polarity to the denticles in the row 3/4 region of *Ser* mutants. Perhaps Ser-dependent Notch activation is also important for the process of denticle shaping per se, though the rescue of row 4 fate that we observed simply by adding back excess *rho* argues against this (Fig. 5; see also next section).

### Fringe and developmental boundaries

Another role suggested for Ser–Notch signaling was that it created a boundary within the denticle field (Alexandre et al., 1999). With our finding that *fng* has an important role in denticle patterning, this idea becomes more satisfying, as *fng* function is closely associated with the establishment of boundaries during development (Irvine and Wieschaus, 1994; Papayannopoulos et al., 1998). However, as noted by Alexandre et al. (1999), the correlation in *rho* and *Ser*

gene expression with polarity changes in the denticle field still needed to be tested. In fact, restoring high level Rho expression in a *Ser* mutant led to restoration of anteriorly pointing row 4 denticles. A developmentally important boundary may yet exist between cell rows 4 and 5, where there is a reversal of denticle polarity. However, if a boundary exists, Ser-dependent Notch signaling is not essential to its formation but may solely be necessary for proper levels of *rho* expression. Thus, the questions of what might constitute this developmental boundary and how a reversal in denticle polarity comes about remain, as yet, unanswered.

*Fringe tempers Serrate-dependent signaling in Notch-active cells*

Our data also do not fit simply with the idea of *fng* establishing the boundaries for where Notch can be activated by Ser. *Ser* is expressed in prospective rows 5–7. While Notch is activated in anteriorly flanking cells (the discrete stripe), and also in posteriorly flanking cells (the broad domain), Notch activation was largely absent from Ser-expressing cells. If the primary role of *fng* was to down-regulate Notch activation by Ser in *Ser*-expressing cells, in *fng* mutant embryos one would now expect an unbroken swath of Notch activation from the discrete stripe through the broad domain. This was not the case, as we still observed the discrete stripe and the broad band separated by about three cell rows with little or no Notch reporter activity; these are likely the *Ser*-expressing cells. Thus, the primary role of *fng* is not to set the boundary of Notch activation by Ser. This contrasts with the well-known role for *fng* in developing wing imaginal disks, where it is essential for a boundary of *Ser*-dependent Notch activation (Irvine and Rauskolb, 2001). In ventral epidermis, perhaps an explanation for the block to Notch activation in the *Ser*-expressing cells may lie in auto-inhibition by high-level ligand expression observed in some tissues (Micchelli et al., 1997).

We did observe a change in Notch reporter expression in *fng* mutants, and this yields a clue to a perhaps novel role played by *fng* in this tissue. We observed increased levels of Notch activity in *fng* mutants, but the increases were in the normal domains of Notch activation. We draw two inferences from this observation. First, since current models strongly suggest a cell autonomous role for *fng* in modifying the Notch receptor, we conclude that there is a physiologically relevant level of *fng* expressed in the cells anterior to the *Ser* domain (and, likely, posterior, also). These are the cells receiving Ser input, and thus there must be *fng*-dependent modifications to the Notch receptor displayed on these cells. The second, and perhaps more important inference we draw from this work, is that *fng* may be playing an important temporal role in patterning the ventral epidermis, rather than a boundary role. *fng* expression is delayed relative to *Ser* expression. Perhaps its role is to temporally dampen Ser-dependent Notch activation so that there is not too high a level of *rho* induction.

## Appendix A. Supplementary data

Supplementary data associated with this article can be found, in the online version, at doi:10.1016/j.ydbio.2005.06.031.

## References

Alexandre, C., Lecoutois, M., Vincent, J.-P., 1999. Wingless and Hedgehog pattern *Drosophila* denticle belts by regulating the production of short-range signals. Development 126, 5689–5698.

Bachmann, A., Knust, E., 1998. Dissection of *cis*-regulatory elements of the *Drosophila* gene Serrate. Dev. Genes Evol. 208 (6), 346–351.

Bruckner, K., Perez, L., Clausen, H., Cohen, S., 2000. Glycosyltransferase activity of Fringe modulates N-Delta interactions. Nature 406 (6794), 411–415.

Couso, J.P., Martinez-Arias, A., 1994. Notch is required for wingless signalling in the epidermis of *Drosophila*. Cell 79, 259–272.

de Celis, J.F., Tyler, D.M., de Celis, J., Bray, S.J., 1998. Notch signalling mediates segmentation of the *Drosophila* leg. Development 125 (23), 4617–4626.

Dubois, L., Lecourtois, M., Alexandre, C., Hirst, E., Vincent, J.P., 2001. Regulated endocytic routing modulates wingless signaling in *Drosophila* embryos. Cell 105 (5), 613–624.

Go, M.J., Artavanis-Tsakonas, S., 1998. Cell proliferation control by Notch signaling in *Drosophila* development. Development 125 (11), 2031–2040.

Golembo, M., Raz, E., Shilo, B.Z., 1996. The *Drosophila* embryonic midline is the site of Spitz processing, and induces activation of the EGF receptor in the ventral ectoderm. Development 122 (11), 3363–3370.

Gritzan, U., Hatini, V., DiNardo, S., 1999. Mutual antagonism between signals secreted by adjacent wingless and engrailed cells leads to specification of complementary regions of the *Drosophila* parasegment. Development 126 (18), 4107–4115.

Hatini, V., DiNardo, S., 2001a. Divide and conquer: pattern formation in *Drosophila* embryonic epidermis. Trends Genet. 17 (10), 574–579.

Hatini, V., DiNardo, S., 2001b. Distinct signals generate repeating striped pattern in the embryonic parasegment. Mol. Cell 7 (1), 151–160.

Hatini, V., Bokor, P., Goto-Mandeville, R., DiNardo, S., 2000. Tissue- and stage Specific modulation of wingless signaling by the segment polarity gene lines. Genes Dev. 14 (11), 1364–1376 (In Process Citation).

Irvine, K.D., Rauskolb, C., 2001. Boundaries in development: formation and function. Annu. Rev. Cell Dev. Biol. 17, 189–214.

Irvine, K.D., Wieschaus, E., 1994. fringe, a boundary-specific signaling molecule mediates interactions between dorsal and ventral cells during *Drosophila* wing development. Cell 79, 595–606.

Klien, D.E., Nappi, V.M., Reeves, G.T., Shvartsman, S.Y., Lemmon, M.A., 2004. Argos inhibits epidermal growth factor receptor signaling by ligand sequestration. Nature 430 (7003), 1040–1044.

Lee, J.R., Urban, S., Garvey, C.F., Freeman, M., 2001. Regulated intracellular ligand transport and proteolysis control EGF signal activation in *Drosophila*. Cell 107 (2), 161–171.

Martinez Arias, A., 1993. Development and patterning of the Larval Epidermis of *Drosophila*. In: Bate, M., Martinez Arias, A. (Eds.), The Development of *Drosophila melanogaster*, vol. 1. Cold Spring Harbor Laboratory Press, New York, pp. 517–608.

Micchelli, C.A., Rulifson, E.J., Blair, S.S., 1997. The function and regulation of cut expression on the wing margin of *Drosophila*: Notch, Wingless and a dominant negative role for Delta and Serrate. Development 124 (8), 1485–1495.

Moloney, D.J., Panin, V.M., Johnston, S.H., Chen, J., Shao, L., Wilson, R., Wang, Y., Stanley, P., Irvine, K.D., Haltiwanger, R.S., Vogt, T.F., 2000. Fringe is a glycosyltransferase that modifies Notch. Nature 406 (6794), 369–375.

O'Keefe, L., Dougan, S.T., Gabay, L., Raz, E., Shilo, B.Z., DiNardo, S., 1997. Spitz and Wingless, emanating from distinct borders, cooperate to establish cell fate across the Engrailed domain in the *Drosophila* epidermis. Development 124 (23), 4837–4845.

Papayannopoulos, V., Tomlinson, A., Panin, V.M., Rauskolb, C., Irvine, K.D., 1998. Dorsal–ventral signaling in the *Drosophila* eye. Science 281 (5385), 2031–2034.

Payre, F., Vincent, A., Carreno, S., 1999. ovo/svb integrates Wingless and DER pathways to control epidermis differentiation. Nature 400 (6741), 271–275.

Rebay, I., Rubin, G.M., 1995. Yan functions as a general inhibitor of differentiation and is negatively regulated by activation of the Ras1/MAPK pathway. Cell 81 (6), 857–866.

Szüts, D., Freeman, M., Bienz, M., 1997. Antagonism between EGFR and Wingless signaling in the larval cuticle of *Drosophila*. Development 124, 3209–3219.

Tsruya, R., Schlesinger, A., Reich, A., Gabay, L., Sapir, A., Shilo, B.Z., 2002. Intracellular trafficking by Star regulates cleavage of the *Drosophila* EGF receptor ligand Spitz. Genes Dev. 16 (2), 222–234.

Urban, S., Lee, J.R., Freeman, M., 2001. *Drosophila* rhomboid-1 defines a family of putative intramembrane serine proteases. Cell 107 (2), 173–182.

van der Meer, S., 1977. Optical clean and permanent whole mount preparation for phase contrast microscopy of cuticular structures of insect larvae. Dros. Inf. Serv. 52, 160–161.

Volk, T., 1999. Singling out *Drosophila* tendon cells: a dialogue between two distinct cell types. Trends Genet. 15 (11), 448–453.

Wiellette, E.L., McGinnis, W., 1999. Hox genes differentially regulate Serrate to generate segment-specific structures. Development 126 (9), 1985–1995.